PHYSICAL REVIEW B **90**, 220513(R) (2014)

Exact correlation functions in the cuprate pseudogap phase: Combined effects of charge order and pairing

Rufus Boyack, Chien-Te Wu, Peter Scherpelz, and K. Levin
James Franck Institute, University of Chicago, Chicago, Illinois 60637, USA

(Received 11 November 2014; revised manuscript received 13 December 2014; published 31 December 2014)

There is a multiplicity of charge-ordered, pairing-based, or pair density wave theories of the cuprate pseudogap, albeit arising from different microscopic mechanisms. For mean-field schemes (of which there are many) we demonstrate here that they have precise implications for two-body physics in the same way that they are able to address the one-body physics of photoemission spectroscopy. This follows because the full vertex can be obtained exactly from the Ward-Takahashi identity. As an illustration, we present the spin response functions, finding that a recently proposed pair density wave (Amperean pairing) scheme is readily distinguishable from other related scenarios.

DOI: 10.1103/PhysRevB.90.220513 PACS number(s): 71.45.Lr, 74.72.Kf, 74.25.Jb

Introduction. A number of theories associated with the cuprate pseudogap phase have recently been suggested, based on the now widely observed charge order [1–4]. While the underlying physics may be different, what emerges rather generally are BCS-based pairing theories of the normal state with band-structure reconstruction [5–7]. Distinguishing between theories has mostly been based on angle resolved photoemission spectroscopy (ARPES) [8]. However, the majority of data available for the cuprates involves two-particle properties: for example, the optical absorption [9], diamagnetism [10], quasiparticle interference in scanning tunneling microscopy (STM) [11], neutron [4,12,13], and inelastic x-ray scattering in the charge [3] and spin [14] sectors.

In this Rapid Communication we use the Ward-Takahashi identity (WTI) [15,16] to develop precise two-body response functions for these pairing-based pseudogap theories. Such exact response functions make it possible to address two-particle cuprate experiments, including the list above, from the perspective of many different theories. As an illustration, we compute the spin-spin correlation functions relevant to neutron scattering in three pseudogap scenarios. That the response functions analytically satisfy the f-sum rule provides the confidence that there are no missing Feynman diagrams or significant numerical inaccuracies.

By comparing the Amperean pairing scheme [6], and that of Yang, Rice, and Zhang [7] with a simple d-wave pseudogap scenario, we find that the Amperean theory leads to a relatively featureless neutron cross section in contrast to the peaks (at and near the antiferromagnetic wave vector), found for the other two theories.

In this Amperean pairing scheme [6] the mean-field self-energy is

$$\Sigma_{\rm pg}(K) = \frac{\Delta_1^2}{\omega + \xi_{\mathbf{k}-\mathbf{p}} - \frac{\Delta_2^2}{\omega - \xi_{\mathbf{k}-2\mathbf{p}}}} + \frac{\Delta_2^2}{\omega + \xi_{\mathbf{k}+\mathbf{p}} - \frac{\Delta_1^2}{\omega - \xi_{\mathbf{k}+2\mathbf{p}}}} + \frac{C_1^2}{\omega - \xi_{\mathbf{k}+2\mathbf{p}} - \frac{\Delta_1^2}{\omega + \xi_{\mathbf{k}+\mathbf{p}}}} + \frac{C_2^2}{\omega - \xi_{\mathbf{k}-2\mathbf{p}} - \frac{\Delta_2^2}{\omega + \xi_{\mathbf{k}-\mathbf{p}}}}. \quad (1)$$

We single out this particular theory as an example which is complex and therefore somewhat more inclusive. In Eq. (1) $\Sigma_{\rm pg}(K)$ is expressed in terms of two different finite momentum ($\mathbf{p}$) pseudogaps, $\Delta_1 \equiv \Delta_{\mathbf{p}}$ and $\Delta_2 \equiv \Delta_{-\mathbf{p}}$. In addition, we have introduced charge density wave (CDW) amplitudes C_1 and C_2. From the self-energy, the full (inverse) Green's function can be deduced: $G^{-1}(K) \equiv G_0^{-1}(K) - \Sigma_{\rm pg}(K) = \omega - \xi_{\mathbf{k}} - \Sigma_{\rm pg}(K)$. This then determines the renormalized band structure, which can be compared with ARPES experiments. One can similarly add other mean-field contributions such as that related to a spin density wave (SDW) [17] or even a d-density wave (DDW) [18].

It is observed from Eq. (1) that in the Amperean pairing case a BCS-like self-energy appears in a continued fraction form within the self-energy itself. There are analogies with the approach of Yang, Rice, and Zhang (YRZ) [7] in the limit that only one gap term is present, say, Δ_1, and when the CDW ordering is absent. Importantly, this single-gap self-energy involves two types of dispersion relations, so that the pairing term leads to pockets or a reconstruction of the band structure. For a simpler d-wave pseudogap, with a single-gap model, both of these dispersion relations are taken to be the same, as was studied microscopically [19] and phenomenologically [20]. A central contribution of this Rapid Communication is to show how, via two-particle properties, important distinctions between these three different pseudogap theories can be established.

While it is argued to be appropriate for the pseudogap phase [6], the self-energy of Eq. (1) is indistinguishable from that of a superconducting state. It is important, then, to ensure that this form for $\Sigma_{\rm pg}$ does not correspond to an ordered phase. Phase fluctuations have been phenomenologically invoked [5,6] to destroy order. Regardless of this phenomenology there is a quantitative constraint to be satisfied: The absence of a Meissner effect above T_C implies that the zero frequency and zero momentum current-current correlation function satisfies $\overleftrightarrow{P}(0) = -(\frac{n}{m})_{\rm dia} \equiv -2\sum_K \frac{\partial^2 \xi_{\mathbf{k}}}{\partial \mathbf{k} \partial \mathbf{k}} G(K)$, so that there is a precise cancellation between the diamagnetic and paramagnetic current-current correlation functions in the normal state.

Performing integration by parts [21] and using the identity $\partial G(K)/\partial \mathbf{k} = -G^2(K)\partial G^{-1}(K)/\partial \mathbf{k}$ then yields the following expression for $\overleftrightarrow{P}(0)$:

$$\overleftrightarrow{P}(0) = 2\sum_K G^2(K) \left\{ \frac{\partial \xi_{\mathbf{k}}}{\partial \mathbf{k}} + \frac{\partial \Sigma_{\rm pg}(K)}{\partial \mathbf{k}} \right\} \frac{\partial \xi_{\mathbf{k}}}{\partial \mathbf{k}}. \quad (2)$$

Here $K = (\omega, \mathbf{k})$. Given the self-energy from Eq. (1), it is then straightforward to arrive at the quantity $\overleftrightarrow{P}(0)$:

$$\overleftrightarrow{P}(0) = 2\sum_K G^2(K)\left\{\frac{\partial\xi_{\mathbf{k}}}{\partial\mathbf{k}} - \Delta_1^2 G_{1,1}^2(-K)\frac{\partial\xi_{\mathbf{k},2}}{\partial\mathbf{k}} + \Delta_1^2\Delta_2^2 G_{1,1}^2(-K)G_{0,4}^2(K)\frac{\partial\xi_{\mathbf{k},4}}{\partial\mathbf{k}} - \Delta_2^2 G_{1,2}^2(-K)\frac{\partial\xi_{\mathbf{k},1}}{\partial\mathbf{k}} + \Delta_2^2\Delta_1^2 G_{1,2}^2(-K)G_{0,3}^2(K)\frac{\partial\xi_{\mathbf{k},3}}{\partial\mathbf{k}}\right\}\frac{\partial\xi_{\mathbf{k}}}{\partial\mathbf{k}}. \quad (3)$$

For simplicity, throughout the main text we set $C_1 = C_2 = 0$ and present the complete expressions in the Supplemental Material [22]. Here we have defined the following four bare (inverse) Green's functions, $G_{0,i}^{-1}(K) = (\omega - \xi_{\mathbf{k},i})$, $i \in \{1,2,3,4\}$, where $\xi_{\mathbf{k},1} = \xi_{\mathbf{k}+\mathbf{p}}, \xi_{\mathbf{k},2} = \xi_{\mathbf{k}-\mathbf{p}}, \xi_{\mathbf{k},3} = \xi_{\mathbf{k}+2\mathbf{p}}, \xi_{\mathbf{k},4} = \xi_{\mathbf{k}-2\mathbf{p}}$ are four dispersion relations. [The usual bare inverse Green's function is denoted by $G_0^{-1}(K) = \omega - \xi_{\mathbf{k}} = \omega - \epsilon_{\mathbf{k}} + \mu$.] The partially dressed Green's functions (which are neither bare nor full) associated with Eq. (1) are

$$G_{1,1}^{-1}(K) = \omega - \xi_{\mathbf{k},1} - \frac{\Delta_2^2}{\omega + \xi_{-\mathbf{k},4}}, \quad (4)$$

$$G_{1,2}^{-1}(K) = \omega - \xi_{\mathbf{k},2} - \frac{\Delta_1^2}{\omega + \xi_{-\mathbf{k},3}}. \quad (5)$$

In terms of these partially dressed Green's functions, the self-energy in Eq. (1) for the case where $C_1 = C_2 = 0$ has the compact form $\Sigma_{\rm pg}(K) = -\Delta_1^2 G_{1,1}(-K) - \Delta_2^2 G_{1,2}(-K)$. The quantity $\overleftrightarrow{P}(0)$ in Eq. (3) provides a template for the form of the Feynman diagrams that we will find in $\overleftrightarrow{P}(Q)$.

Ward-Takahashi identity (WTI) for the full vertex. The exact expression for the current-current correlation function $\overleftrightarrow{P}(Q)$ is contained in the response functions written as

$$P^{\mu\nu}(Q) = 2\sum_K \Gamma^\mu(\tilde{K},K)G(K)\gamma^\nu(K,\tilde{K})G(\tilde{K}). \quad (6)$$

Throughout the text, we set $\tilde{K} \equiv K + Q$. The full vertex in four-vector notation is given by $\Gamma^\mu(\tilde{K},K) = [\Gamma^0(\tilde{K},K), \mathbf{\Gamma}(\tilde{K},K)]$, where the first argument denotes the incoming momentum and the second argument the outgoing momentum. Here the quantity $\gamma^\nu(K,\tilde{K})$ represents the bare vertex.

The full response kernel is $K^{\mu\nu}(Q) \equiv P^{\mu\nu}(Q) + (\frac{n}{m})^{\mu\nu}_{\rm dia}(1 - \delta_{0,\nu}\delta_{\mu,\nu})$, where there is no summation over indices in the second term. The Ward-Takahashi identity in quantum field theory is a diagrammatic identity that imposes a symmetry between response functions. The particular symmetry we are interested in is the $U(1)_{\rm EM}$ Abelian gauge symmetry [15]. As we shall show, satisfying the WTI also leads to manifestly sum-rule-consistent response functions. Charge conservation is an exact relation between the current-current and density-density response functions that follows from this $U(1)_{\rm EM}$ symmetry. The WTI reflects this charge conservation which imposes the constraint $\Omega K^{0\nu} + i\,{\rm div}_{\mathbf{q}}\, K^{j\nu} = 0$. The WTI for the vertex $\Gamma^\mu(\tilde{K},K)$ on a lattice is

$$\begin{aligned}\Omega\Gamma^0(\tilde{K},K) + i\,{\rm div}_{\mathbf{q}}\,\mathbf{\Gamma}(\tilde{K},K) &= G^{-1}(\tilde{K}) - G^{-1}(K),\\ &= \Omega + i\,{\rm div}_{\mathbf{q}}\,\boldsymbol{\gamma}(\tilde{K},K) + \Sigma_{\rm pg}(K) - \Sigma_{\rm pg}(\tilde{K}).\end{aligned} \quad (7)$$

The WTI for the bare vertex $\gamma^\mu(\tilde{K},K)$ is $\Omega + i\,{\rm div}_{\mathbf{q}}\,\boldsymbol{\gamma} = G_0^{-1}(\tilde{K}) - G_0^{-1}(K) = \Omega - \xi_{\mathbf{k}+\mathbf{q}} + \xi_{\mathbf{k}}$. Similarly we introduce the bare vertices $\gamma_i^\mu(\tilde{K},K)$ associated with the dispersion relations $\xi_{\mathbf{k},i}$. Here ${\rm div}_{\mathbf{q}}\,\mathbf{\Gamma}(\tilde{K},K)$, complicated due to lattice effects, is the Fourier transform of the divergence of $\mathbf{\Gamma}$.

In the limit $Q \to 0$, the Ward-Takahashi identity reduces to the Ward identity, $\delta\Gamma^\mu(K,K) \equiv \Gamma^\mu(K,K) - \gamma^\mu(K,K) = -\partial\Sigma_{\rm pg}(K)/\partial k_\mu$. This is fully consistent with the arguments leading up to the no-Meissner constraint in Eq. (2). In this continuum limit ($q \to 0$), the WTI and charge conservation have familiar forms, $q_\mu\Gamma^\mu(\tilde{K},K) = G^{-1}(\tilde{K}) - G^{-1}(K)$ and $q_\mu K^{\mu\nu}(Q) = 0$, respectively.

We emphasize that, given an arbitrary self-energy, solving the WTI analytically for the full vertex $\Gamma^\mu(\tilde{K},K)$ is generally not possible. However, there is a well-defined procedure to determine this vertex in principle. One inserts the bare vertex in all possible places in the self-energy diagrams and sums the resulting series of diagrams. For the class of theories considered in this Rapid Communication, Σ itself does *not* depend on the full Green's function $G(\Sigma)$, but rather depends on the bare Green's functions G_0 and their simple extensions; this is associated with generalized mean-field theories. For example, in strict BCS theory, $\Sigma(K) = -\Delta^2 G_0(-K)$.

Importantly, it follows that in the BCS-like theories of interest here, the full vertex, $\Gamma^\mu(\tilde{K},K)$, can be deduced from the equivalent WTI by considering only finitely many loop diagrams. We illustrate this procedure specifically for the first term in the Amperean self-energy in Eq. (1). Using the form of the self-energy, along with the bare WTI, we have

$$\begin{aligned}\Sigma_1(K) - \Sigma_1(\tilde{K}) &= \Delta_1^2 G_{1,1}(-K)G_{1,1}(-\tilde{K})\{[\Omega + \xi_{\mathbf{k}+\mathbf{q}-\mathbf{p}} - \xi_{\mathbf{k}-\mathbf{p}}] + \Delta_2^2 G_{0,4}(K)G_{0,4}(\tilde{K})[\Omega - \xi_{\mathbf{k}+\mathbf{q}-2\mathbf{p}} + \xi_{\mathbf{k}-2\mathbf{p}}]\}\\ &= \Delta_1^2 G_{1,1}(-K)G_{1,1}(-\tilde{K})\{[\Omega + i\,{\rm div}_{\mathbf{q}}\,\boldsymbol{\gamma}_1(-K,-\tilde{K})] + \Delta_2^2 G_{0,4}(K)G_{0,4}(\tilde{K})[\Omega + i\,{\rm div}_{\mathbf{q}}\,\boldsymbol{\gamma}_4(\tilde{K},K)]\}\end{aligned} \quad (8)$$

and

$$\begin{aligned}\Omega\Gamma^0(\tilde{K},K) + i\,{\rm div}_{\mathbf{q}}\,\mathbf{\Gamma}(\tilde{K},K) = \Omega + i\,{\rm div}_{\mathbf{q}}\,\boldsymbol{\gamma}(\tilde{K},K) &+ \Delta_1^2 G_{1,1}(-K)G_{1,1}(-\tilde{K})\{[\Omega + i\,{\rm div}_{\mathbf{q}}\,\gamma_1(-K,-\tilde{K})]\\ &+ \Delta_2^2 G_{0,4}(K)G_{0,4}(\tilde{K})[\Omega + i\,{\rm div}_{\mathbf{q}}\,\boldsymbol{\gamma}_4(\tilde{K},K)]\}.\end{aligned} \quad (9)$$

In this form we can then solve for the exact full vertex:

$$\begin{aligned}\Gamma^\mu(\tilde{K},K) = \gamma^\mu(\tilde{K},K) &+ \Delta_1^2 G_{1,1}(-K)G_{1,1}(-\tilde{K})[\gamma_1^\mu(-K,-\tilde{K}) + \Delta_2^2 G_{0,4}(K)G_{0,4}(\tilde{K})\gamma_4^\mu(\tilde{K},K)]\\ &+ \Delta_2^2 G_{1,2}(-K)G_{1,2}(-\tilde{K})\big[\gamma_2^\mu(-K,-\tilde{K}) + \Delta_1^2 G_{0,3}(K)G_{0,3}(\tilde{K})\gamma_3^\mu(\tilde{K},K)\big].\end{aligned} \quad (10)$$

Here we have now included the second term from $\Sigma_{\rm pg}(K)$ in Eq. (1).

We emphasize this is not an expansion in the bare vertices. Rather, the WTI is used to obtain the exact full vertex. The crucial step is that the self-energy does not depend on the full Green's function. If it did, then the full vertex would appear on both sides of the equation, reducing the problem to a Bethe-Salpeter equation [16].

Using the full vertex, the exact response function can then be determined via Eq. (6). The Amperean pairing response functions would have nine associated Feynman diagrams if one considered the charge density wave: one of one-loop order (two Green's functions), four of two-loop order (four Green's functions), and four of three-loop order (six Green's functions). The nine Feynman diagrams contributing to the response functions are presented in the Supplemental Material [22].

The bare vertices for the density component are given by $\gamma^0(\tilde{K},K)=\gamma_i^0(\tilde{K},K)=1$. This then allows the exact density-density response function $P_{\rho\rho}(Q)$ to be computed for all Q. More complicated, for an arbitrary band structure, are the bare vertices that enter into the current-current correlation function. However, in the limit $q\to 0$ these can be determined from Eq. (3). The same reasoning which is used to determine $P_{\rho\rho}(Q)$ for all Q is applicable to the spin (density) response, as measured in neutron experiments.

The full spin response function $P_S^{\mu\nu}(Q)$ is defined by

$$P_S^{\mu\nu}(Q)=\sum_K\sum_\sigma \Gamma^\mu_{S_\sigma}(\tilde{K},K)G(K)\gamma^\nu_{S_\sigma}(K,\tilde{K})G(\tilde{K}). \tag{11}$$

Here the bare spin vertex is denoted by $\gamma^\mu_{S_\sigma}(\tilde{K},K)$, where $S_\sigma=\pm1$ and $S_{\bar\sigma}=-S_\sigma$. The bare WTI for the spin vertex is $\Omega+i\,{\rm div}_{\mathbf{q}}\boldsymbol{\gamma}_{S_\sigma}=S_\sigma(G_0^{-1}(\tilde{K})-G_0^{-1}(K))=S_\sigma(\Omega-\xi_{\mathbf{k}+\mathbf{q}}+\xi_{\mathbf{k}})$. Similarly the full WTI for the full spin vertex $\Gamma^\mu_{S_\sigma}(\tilde{K},K)$ is

$$\Omega\Gamma^0_{S_\sigma}+i\,{\rm div}_{\mathbf{q}}\boldsymbol{\Gamma}_{S_\sigma}=S_\sigma(G^{-1}(\tilde{K})-G^{-1}(K)). \tag{12}$$

We can then read off the spin-spin correlation function directly using Eq. (10).

From the established constraints on the bare and full vertices one can directly derive [23] the f-sum rule for the density-density and spin density response functions,

$$\int\frac{d\omega}{\pi}(-\omega\,{\rm Im}\,P^{00}(Q))=2\sum_{\mathbf{k}}n_{\mathbf{k}}[\xi_{\mathbf{k}+\mathbf{q}}+\xi_{\mathbf{k}-\mathbf{q}}-2\xi_{\mathbf{k}}], \tag{13}$$

where $n_{\mathbf{k}}=T\sum_{i\omega}G(K)$. Importantly, this sum rule (and counterparts for the current-current correlation function) is satisfied exactly provided the response functions are consistent with the WTI. This is discussed in more detail in the Supplemental Material [22].

Behavior of the neutron cross section: Comparison of pseudogap theories. For illustrative purposes we focus on the spin-density response function, conventionally called $\chi_0(Q)$. Importantly, ensuring Eq. (13) is satisfied provides tight control over numerical calculations of this correlation function. When no simplifications are introduced, our numerical calculations agree with the sum rule to an accuracy of the order of 0.1%–0.2% [21] in all three models. The quantity ${\rm Im}\,\chi_0(Q)\equiv-{\rm Im}\,P^{00}(Q)$ is the theoretical basis for neutron scattering experiments. [Note that we adopt the sign convention for the density correlation functions $P_{\rho\rho}(Q)=P^{00}(Q)$ for spin and charge.]

For simple d-wave pairing models, a very reasonable comparison between theory and neutron data has been reported at high temperatures (where one sees a reflection of the fermiology [24,25]) and below T_C (where one sees both a commensurate (π,π) [26] and a slightly incommensurate frequency-dependent "hourglass" structure [27,28]). This approach to neutron scattering presents a (rather successful) rival scheme to stripe approaches; many different theories, built on different microscopics, have arrived at similar behavior [29–32]. In the pseudogap phase (which has received less attention theoretically), there are peaks at and near (π,π) [4,12,13] which have been recently argued [4] to reflect some degree of broken orientational symmetry.

Here we compare the results for $\chi_0(Q)$ using three different theories of the pseudogap: a simple d-wave pseudogap, the theory of Yang, Rice, and Zhang, and that of Amperean pairing. For the Amperean case we follow Ref. [6] and consider the simpler 3×3 reduced Hamiltonian. In this 3×3 form,

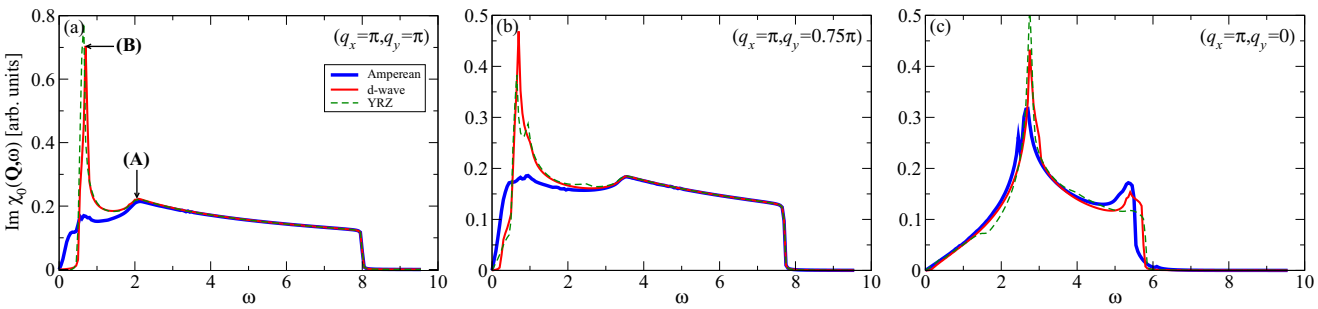

FIG. 1. (Color online) Comparison of the spin density correlation function ${\rm Im}\,\chi_0(Q)=-{\rm Im}\,P_S^{00}(\omega,\mathbf{q})$ for three different values of $\mathbf{q}$ in the Amperean, d-wave, and YRZ pseudogap theories. In (a) we have labeled the van Hove peaks appearing in the d-wave theory, which appear as saddle points in the contour plot of Fig. 2. Here we use the band structure given in Ref. [3] with $T=0.01$ and a broadening of $\Gamma=0.01$. The doping $p=0.12$ and the chemical potential μ is fixed by the Luttinger sum rule. The band structure and frequency are all normalized by t, and the gap function has an amplitude of $\Delta_0=0.15$. For the Amperean theory we use a k_x,k_y-symmetrized Gaussian [6] gap function.

$C_1 = C_2 = 0$ and terms involving $\xi_{\mathbf{k}\pm 2\mathbf{p}}$ are dropped. We do not include the effects of the widely used random phase approximation (RPA) enhanced denominator introduced in Ref. [33]. In the RPA enhanced form, $\chi(Q) = \chi_0(Q)/[1 + J(Q)\chi_0(Q)]$, where $J(Q)$ is an effective exchange. Even though $\chi_0(Q)$ is exact, introducing this ratio will lead to a violation of the f-sum rule; this effect is not central to distinguishing between theories, as is our goal here.

Figure 1 presents a plot of Im $\chi_0(Q)$, for three fixed $\mathbf{q}$ corresponding to (π,π) in Fig. 1(a), $(\pi,0.75\pi)$ in Fig. 1(b), and $(\pi,0)$ in Fig. 1(c) as functions of ω. The normal state (above T^*) band structure is taken to be the same, as is the pseudogap amplitude. The behavior in the low ω regime is principally, but not exclusively, dominated by the effects of the gap, while at very high ω the behavior is band-structure dominated. Importantly, all theories essentially converge once ω is much larger than the gap. This means that interesting effects associated with high energy scales [14], such as observed in recent resonant inelastic x-ray scattering (RIXS) experiments, would not be specific to a given theory.

Figure 1 shows that there is little difference in the spin dynamics between the approach of YRZ [7] and that of a d-wave pseudogap, emphasized earlier in a different context [34], and helps to explain the literature claims of successful reconciliation with the data that surround both scenarios [27,28,32].

What appears most distinctive is the Amperean pairing response function, particularly away from $\mathbf{q} = (\pi,0)$. Notable here is the absence of the sharp van Hove peak (marked by B in Fig. 1) which appears in both of the other theories and which is ultimately responsible for commensurate peaks or neutron resonance effects [26]. Also missing from the Amperean scenario is the so-called spin gap, apparent at (π,π) in both of the other two theories. Rather, for Amperean pairing there are multiple low energy processes which contribute to the spin density correlation function.

To better understand these processes, in Fig. 2 we probe the dominant component of the integrand in Im $\chi_0(Q)$ near $\mathbf{q} = (\pi,\pi)$ for the Amperean (right) as compared with d-wave pseudogap (left) scenarios. We show the equal energy contours for the sum of the quasiparticle dispersions, $E_2(\mathbf{k}) \equiv E_{\mathbf{k}} + E_{\mathbf{k}+\mathbf{q}}$ vs k_x and k_y in the pseudogap state [35]. Indicated on the figure are the van Hove singularities A and B (saddle points in the contour plot), as labeled in Fig. 1(a). The lower energy van Hove point (point B) is clearly suppressed in the Amperean pairing case, while it is very pronounced

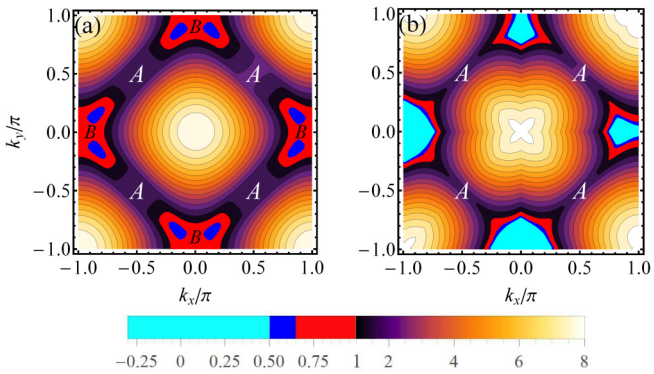

FIG. 2. (Color online) The equal energy contours $E_2(\mathbf{k}) \equiv E_{\mathbf{k}} + E_{\mathbf{k}+\mathbf{q}}$ which appear as the integrand in Im $\chi_0(\omega,\mathbf{q})$ for both (a) d-wave and (b) the Amperean pseudogap schemes. Here $\mathbf{q} = (\pi,\pi)$. Note there are several energy scales, as indicated by the legend. The labels A and B indicate the location of the saddle points of Im $\chi_0(\mathbf{q},\omega)$.

and found to be important [28] for the d-wave case. Also evident from the cyan region in Fig. 2 is the absence of a low ω minimum (spin gap) in $E_2(\mathbf{k})$, as found in both of the other two theories, as well as in the integrated response function.

Conclusions. The central contribution of this Rapid Communication has been to establish an analytically and numerically controlled methodology for addressing the long list of two-particle cuprate measurements. Given a mean-field-like self-energy, the exploitation of the Ward-Takahashi identity (and related sum rules) allows one to evaluate two-particle properties, and in this way achieve the same level of accuracy in these comparisons, as in, say, ARPES. To demonstrate the utility of this method, we address the spin density response functions of neutron scattering and have singled out signatures of the recently proposed Amperean pairing theory [6]. We cannot firmly establish that this pair density wave theory is inconsistent with experiments (without digressing from our goals and including the sum-rule-inconsistent RPA enhancement denominator [33]), but it does lead to a rather featureless neutron cross section [36]. We report two distinctive observations: the absence of both spin gap effects and of the sharp van Hove peaks near (π,π).

This work is supported by NSF-MRSEC Grant No. 0820054. We are grateful to A.-M. S. Tremblay, Yan He, and Adam Rançon for helpful conversations.

[1] G. Ghiringhelli *et al.*, Science **337**, 821 (2012).
[2] W. D. Wise, M. C. Boyer, K. Chatterjee, T. Kondo, T. Takeuchi, H. Ikuta, Y. Wang, and E. W. Hudson, Nat. Phys. **4**, 696 (2008).
[3] R. Comin *et al.*, Science **343**, 390 (2014).
[4] V. Hinkov, P. Bourges, S. Pailhès, Y. Sidis, A. Ivanov, C. D. Frost, T. G. Perring, C. T. Lin, D. P. Chen, and B. Keimer, Nat. Phys. **3**, 780 (2007).
[5] H.-D. Chen, O. Vafek, A. Yazdani, and S.-C. Zhang, Phys. Rev. Lett. **93**, 187002 (2004).
[6] P. A. Lee, Phys. Rev. X **4**, 031017 (2014).
[7] K.-Y. Yang, T. M. Rice, and F.-C. Zhang, Phys. Rev. B **73**, 174501 (2006).
[8] A. Damascelli, Z. Hussain, and Z.-X. Shen, Rev. Mod. Phys. **75**, 473 (2003).
[9] J. Corson, R. Mallozzi, J. Orenstein, J. N. Eckstein, and I. Bozovic, Nature (London) **398**, 221 (1999).
[10] L. Li, Y. Wang, S. Komiya, S. Ono, Y. Ando, G. D. Gu, and N. P. Ong, Phys. Rev. B **81**, 054510 (2010).
[11] S. H. Pan, E. W. Hudson, A. K. Gupta, K.-W. Ng, H. Eisaki, S. Uchida, and J. C. Davis, Phys. Rev. Lett. **85**, 1536 (2000).

[12] C. Stock, W. J. L. Buyers, R. Liang, D. Peets, Z. Tun, D. Bonn, W. N. Hardy, and R. J. Birgeneau, Phys. Rev. B **69**, 014502 (2004).
[13] P. Dai, H. A. Mook, S. M. Hayden, G. Aeppli, T. G. Perring, R. D. Hunt, and F. Doğan, Science **284**, 1344 (1999).
[14] M. L. Tacon *et al.*, Nat. Phys. **7**, 725 (2011).
[15] L. H. Ryder, *Quantum Field Theory*, 2nd ed. (Cambridge University Press, Cambridge, UK, 1996).
[16] J. R. Schrieffer, *Theory of Superconductivity*, 1st ed. (W. A. Benjamin, New York, 1964).
[17] D. Podolsky, E. Demler, K. Damle, and B. I. Halperin, Phys. Rev. B **67**, 094514 (2003).
[18] S. Chakravarty, R. B. Laughlin, D. K. Morr, and C. Nayak, Phys. Rev. B **63**, 094503 (2001).
[19] Q. J. Chen, J. Stajic, S. N. Tan, and K. Levin, Phys. Rep. **412**, 1 (2005).
[20] M. R. Norman, M. Randeria, H. Ding, and J. C. Campuzano, Phys. Rev. B **57**, R11093(R) (1998).
[21] For simplicity in the text, we will ignore terms that arise from the wave vector dependence of the d-wave gap function. In general, this is a small effect. We can see via the sum-rule accuracy the importance of including the full wave vector dependence of the d-wave gap. When the wave vector dependence of the gap is ignored, the sum-rule accuracy is still very good, but now of the order of 2%–3%.
[22] See Supplemental Material at http://link.aps.org/supplemental/10.1103/PhysRevB.90.220513 for complete expressions of the response functions including charge density wave contributions. It also presents a proof of the various sum rules and discusses the extension to the spin response channel.
[23] D. Bergeron, V. Hankevych, B. Kyung, and A.-M. S. Tremblay, Phys. Rev. B **84**, 085128 (2011).
[24] Q. Si, Y. Zha, K. Levin, and J. P. Lu, Phys. Rev. B **47**, 9055 (1993).
[25] Y. Zha, Q. Si, and K. Levin, Physica C **212**, 413 (1993).
[26] D. Z. Liu, Y. Zha, and K. Levin, Phys. Rev. Lett. **75**, 4130 (1995).
[27] Y. Zha, K. Levin, and Q. Si, Phys. Rev. B **47**, 9124 (1993).
[28] Y.-J. Kao, Q. M. Si, and K. Levin, Phys. Rev. B **61**, R11898(R) (2000).
[29] G. Stemmann, C. Pépin, and M. Lavagna, Phys. Rev. B **50**, 4075 (1994).
[30] J. Brinckmann and P. A. Lee, Phys. Rev. Lett. **82**, 2915 (1999).
[31] M. R. Norman, Phys. Rev. B **61**, 14751 (2000).
[32] A. J. A. James, R. M. Konik, and T. M. Rice, Phys. Rev. B **86**, 100508(R) (2012).
[33] Q. Si, J. P. Lu, and K. Levin, Phys. Rev. B **45**, 4930 (1992).
[34] P. Scherpelz, A. Rançon, Y. He, and K. Levin, Phys. Rev. B **90**, 060506(R) (2014).
[35] For the 3×3 Amperean theory, we chose the top band for both $E_{\mathbf{k}}$ and $E_{\mathbf{k}+\mathbf{q}}$.
[36] In addition to the Gaussian gap model of Ref. [6], we have found similar featureless results for a simple d-wave gap shape as well.